Report

Current Biology

Bacterial Infection Disrupts Clock Gene Expression to Attenuate Immune Responses

Graphical Abstract

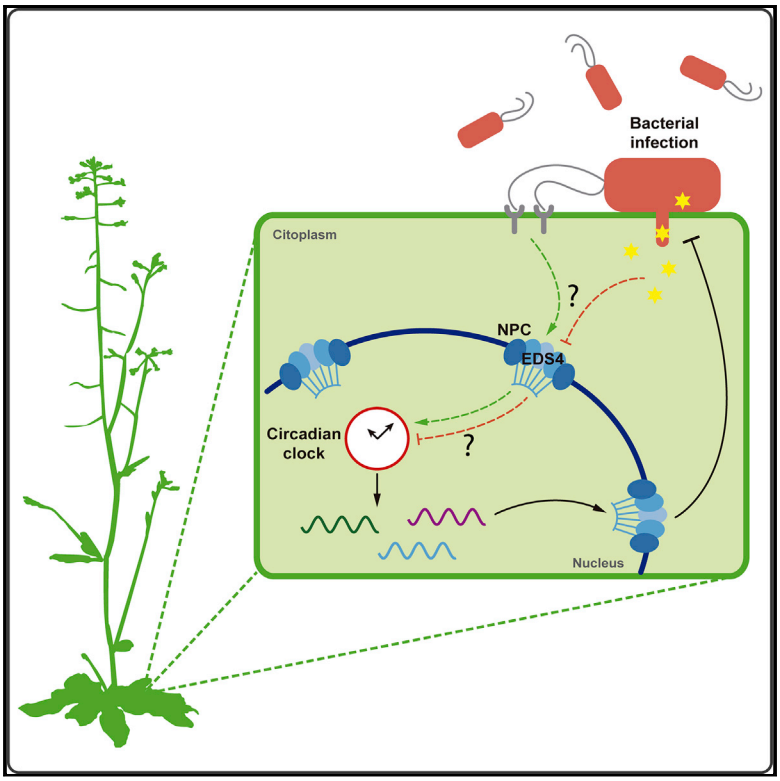

Authors

María José de Leone,
C. Esteban Hernando,
Andrés Romanowski, ...,
Martín Vázquez,
Korbinian Schneeberger,
Marcelo J. Yanovsky

Correspondence

myanovsky@leloir.org.ar

In Brief

Little is known regarding the mechanisms involved in the clock-immunity crosstalk. de Leone et al. report that the defense mutant *eds4* carries a mutation in *NUCLEOPORIN205* which affects its circadian function, and that leads to an attenuation of the transcriptional reprogramming in core clock genes that take place soon after a bacterial infection.

Highlights

- *eds4* mutants display alterations in light and clock-regulated processes
- A mutation in the *NUCLEOPORIN205* gene is responsible for the *eds4* phenotype
- *EDS4* impacts on gene expression and nuclear to total mRNA levels of clock genes
- Bacterial infection downregulates clock genes, and this effect is attenuated in *eds4*

de Leone et al., 2020, Current Biology *30*, 1740–1747
May 4, 2020
https://doi.org/10.1016/j.cub.2020.02.058

CellPress

CellPress

Current Biology
Report

Bacterial Infection Disrupts Clock Gene Expression to Attenuate Immune Responses

María José de Leone,[1] C. Esteban Hernando,[1,6] Andrés Romanowski,[2,6] Daniel A. Careno,[1] Ana Faigón Soverna,[1] Hequan Sun,[3] Nicolás G. Bologna,[4] Martín Vázquez,[5] Korbinian Schneeberger,[3] and Marcelo J. Yanovsky[1,7,*]

[1]Fundación Instituto Leloir, Instituto de Investigaciones Bioquímicas de Buenos Aires–Consejo Nacional de Investigaciones Científicas y Técnicas (CONICET), C1405BWE Buenos Aires, Argentina
[2]Institute for Molecular Plant Sciences, School of Biological Sciences, University of Edinburgh, Edinburgh EH9 3BF, UK
[3]Department of Plant Developmental Biology, Max Planck Institute for Plant Breeding Research, Cologne 50829, Germany
[4]Center for Research in Agricultural Genomics (CRAG), Barcelona 08193, Spain
[5]Instituto de Agrobiotecnología de Rosario (INDEAR), CONICET, S2000EZP Rosario, Argentina
[6]These authors contributed equally
[7]Lead Contact
*Correspondence: myanovsky@leloir.org.ar
https://doi.org/10.1016/j.cub.2020.02.058

SUMMARY

The circadian clock modulates immune responses in plants and animals; however, it is unclear how host-pathogen interactions affect the clock. Here we analyzed clock function in *Arabidopsis thaliana* mutants with defective immune responses and found that *enhanced disease susceptibility 4* (*eds4*) displays alterations in several circadian rhythms. Mapping by sequencing revealed that *EDS4* encodes the ortholog of *NUCLEOPORIN 205*, a core component of the inner ring of the nuclear pore complex (NPC). Consistent with the idea that the NPC specifically modulates clock function, we found a strong enrichment in core clock genes, as well as an increased nuclear to total mRNA accumulation, among genes that were differentially expressed in *eds4* mutants. Interestingly, infection with *Pseudomonas syringae* in wild-type (WT) plants downregulated the expression of several morning core clock genes as early as 1 h post-infection, including all members of the *NIGHT LIGHT-INDUCIBLE AND CLOCK-REGULATED* (*LNK*) gene family, and this effect was attenuated in *eds4*. Furthermore, *lnk* mutants were more susceptible than the WT to *P. syringae* infection. These results indicate that bacterial infection, acting in part through the NPC, alters core clock gene expression and/or mRNA accumulation in a way that favors bacterial growth and disease susceptibility.

RESULTS AND DISCUSSION

There is growing evidence that biotic stress responses are regulated by the circadian clock in plants [1] and that pathogen attacks somehow affect circadian oscillations [2–4]. To better understand the interactions between immune and circadian signaling networks, we evaluated whether *Arabidopsis thaliana* mutants known to have compromised immune responses also display alterations in light- and/or clock-regulated processes. We analyzed light inhibition of hypocotyl elongation and circadian rhythms in leaf movements of several *Arabidopsis thaliana* mutants with increased susceptibility to pathogen infection [5–8] and found that the *enhanced disease susceptibility 4* (*eds4)* mutant had altered responses compared to wild-type (WT) plants in both physiological assays (Figures S1A and S1B). Specifically, hypocotyl elongation in *eds4* was less sensitive than in WT to red and white (but not blue) light, suggesting that EDS4 modulates the activity of the phytochrome photoreceptor signaling pathway (Figures 1A–1C). Flowering time, which is also regulated by the clock [9], was accelerated in *eds4* compared to WT plants (Figure 1D). Furthermore, the circadian leaf movements of *eds4*, but not of the other mutants, had a longer period compared to WT plants (Figures 1E and S1B). Similarly, circadian period and expression profiles of clock genes were also altered in *eds4* (Figure 1E). Together, these data show that, in addition to the enhanced disease susceptibility phenotype, *eds4* shows photomorphogenic, flowering time, and circadian rhythm defects.

The *eds4* mutant was identified more than 20 years ago in a screen of ethyl methanesulfonate (EMS)-mutagenized *Arabidopsis thaliana* plants for individuals that were more susceptible to infection with *Pseudomonas syringae Psm* ES4326, and it was characterized as a single recessive mutation [8]. However, attempts to map the underlying mutation failed due to unclear segregation patterns of the disease phenotype when *eds4,* isolated in the Columbia accession, was outcrossed to other accessions [10]. By combining mapping by sequencing with classical segregation analysis in an F2 population of *eds4* mutants backcrossed to the Columbia WT, we determined that the mutation responsible for the clock phenotype of *eds4* was located on chromosome 5, position 20818109. The mutation consists of a nonsynonymous transition (C→T) that replaces a codon specifying a glutamine residue (CAG) with a premature stop codon (TAG) in *NUCLEOPORIN 205* (*NUP205*) (Figure 2A). This results in a truncated protein version of NUP205 (also known as EMB3142, At5g51200).

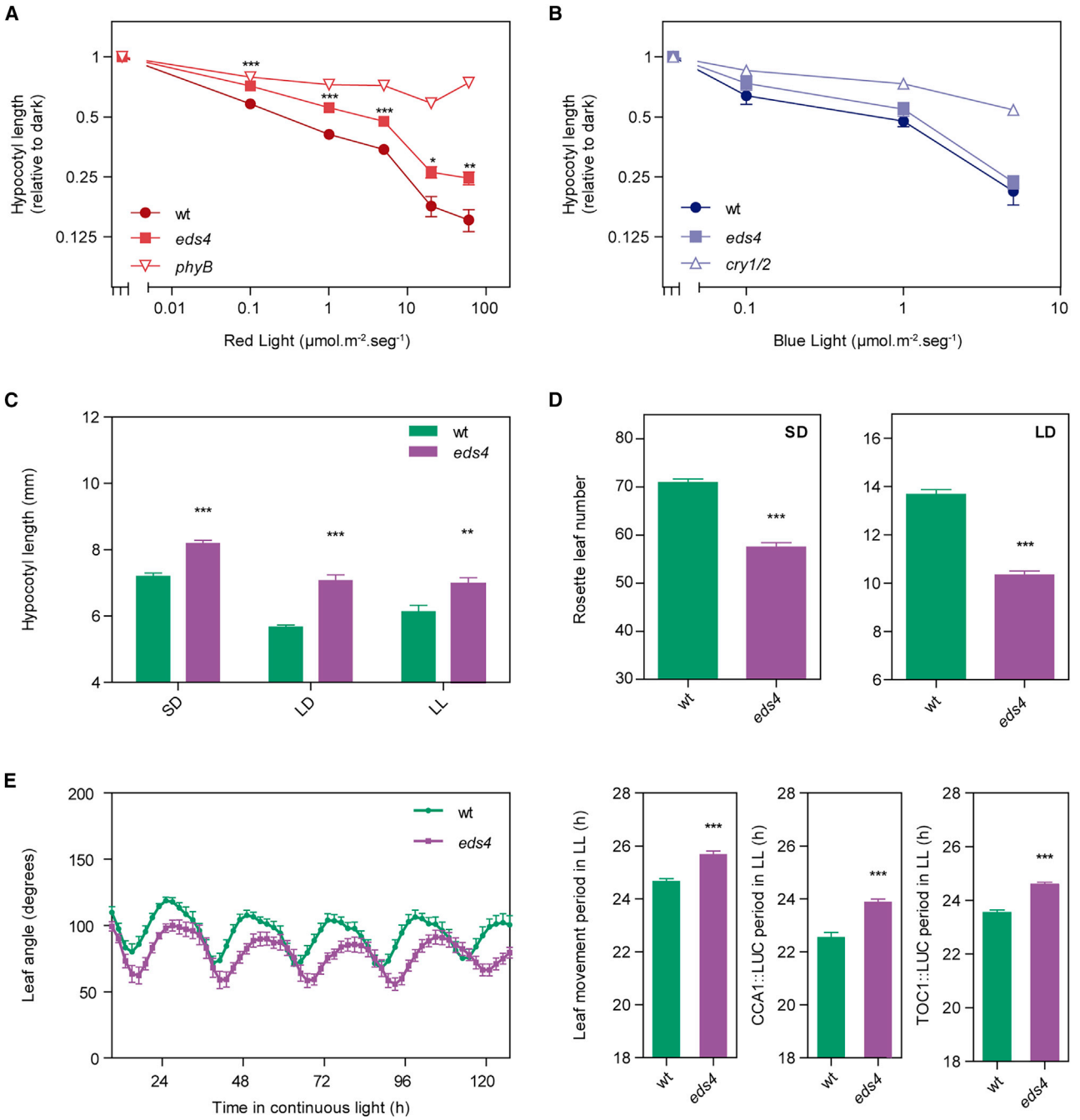

Figure 1. Physiological Characterization of the *Enhanced Disease Susceptibility 4* Mutant

(A and B) Hypocotyl length of seedlings grown under continuous red (A) or blue (B) light relative to the length of the hypocotyl of seedlings grown in darkness (n = 6 replicates of 10 seedlings each). *phyb:* Phytochrome B null mutant, *cry1/2:* Cryptochrome 1 and Cryptochrome 2 double mutant. See also Figure S1A.

(C) Hypocotyl length of seedlings grown under short-day (SD) photoperiods, long-day (LD) photoperiods, or continuous white light (LL) (n = 6 replicates of 10 seedlings each).

(D) Flowering time measured as the number of rosette leaves at bolting in SD (n = 2 independent experiments of 12 plants each) and LD photoperiods (n = 3 independent experiments of 12 plants each).

(E) Circadian rhythms in constant white light after entrainment under LD conditions. For the leaf movement assays (left), leaf angles were measured for the first pair of leaves in 10-day-old seedlings (n = 10 plants). These experiments were repeated at least three times with similar results. See also Figure S1B. In the bioluminescence assays (right), pCCA1::LUC and pTOC1::LUC activity was recorded every hour over 5 days in seedlings that were 5 days old at the start of the experiment (n = 6 plants). These experiments were repeated at least two times with similar results. Periods of circadian rhythms were estimated by fast Fourier transform-non-linear least-squares (FFT-NLLS) algorithm with BRASS 3.0 software. Error bars indicate SEM. *p < 0.05; **p < 0.01; ***p < 0.001 (Student's t test).

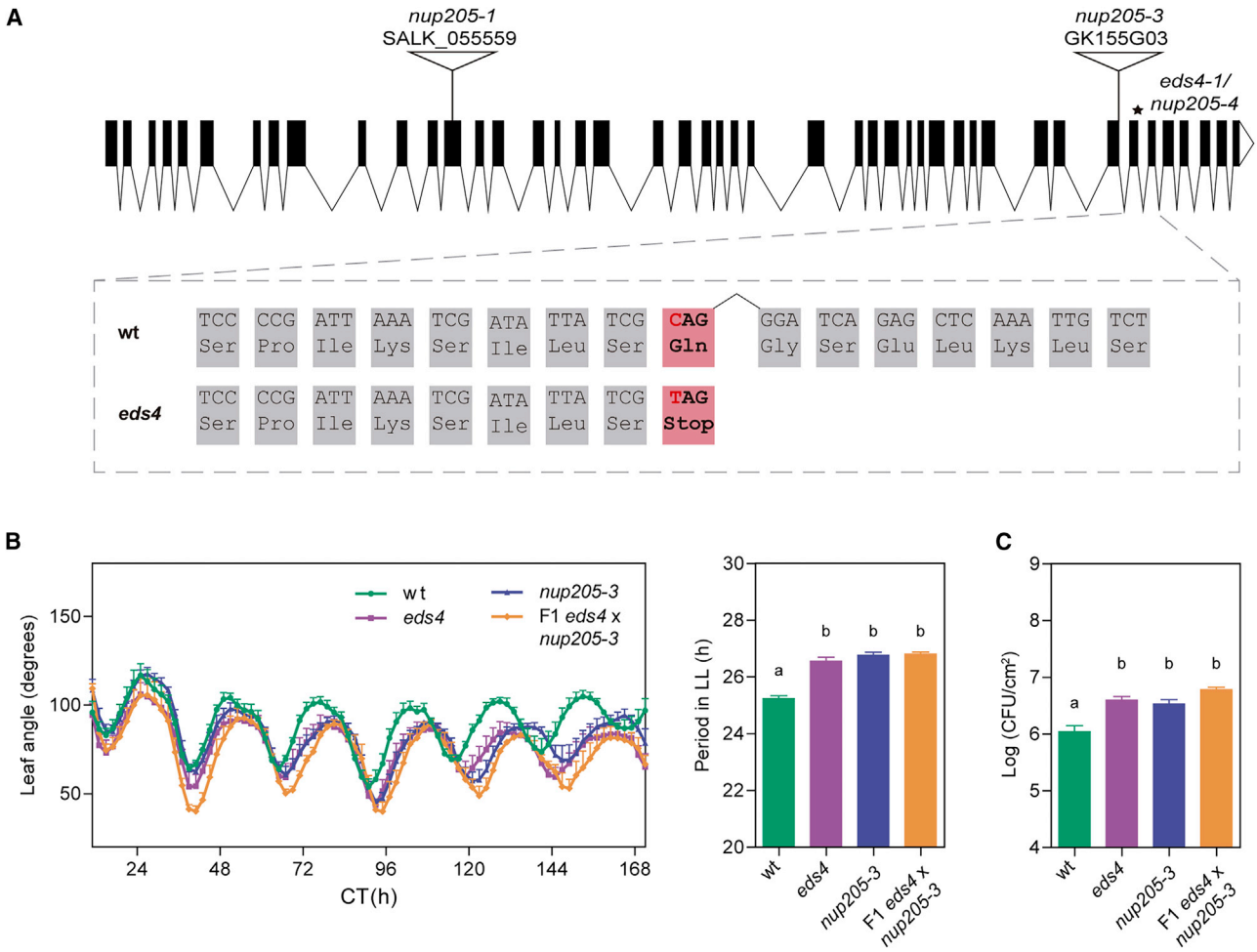

Figure 2. The *eds4* Mutant Carries a Point Mutation in NUP205, a Member of the Nuclear Pore Complex

(A) Schematic representation of the *eds4/nup205* mutations across the *NUP205* locus. Exons are shown as black boxes and introns as black lines. The *eds4* point mutation position is marked with an asterisk, and T-DNA insertions of other mutant alleles are labeled and represented as triangles. The *eds4* mutation introduces a single nucleotide polymorphism that inserts a premature stop codon (TAG) instead of a glutamine (CAG). See also Data S1.

(B) Leaf angles and associated period measured for the first pair of leaves in plants entrained under LD conditions and then transferred to constant light (n = 5 plants) in WT, *eds4*, *nup205-3*, and F1 plants produced by a cross between *eds4* and *nup205-3* mutants. See also Figure S1. This experiment was repeated at least three times with similar results. Periods of circadian rhythms were estimated by FFT-NLLS algorithm with BRASS 3.0 software.

(C) 5- to 6-week-old plants grown in SD conditions were infected by infiltration with *Psm* ES4326. Bacterial growth was assessed 2 d.p.i. (CFU: colony-forming units) in WT, *eds4*, *nup205-3*, and F1 plants. Data represent the average of log-transformed bacterial growth (n = 8 independent biological replicates). This experiment was repeated twice with similar results. Error bars indicate SEM. Different letters indicate significant difference among genotypes, $p < 0.05$ (One-way ANOVA followed by Tukey's multi-comparison test). See also Figure S2.

To verify the identity of the *eds4* mutant, we obtained two additional *nup205* mutant lines (Figure 2A). We found that *nup205-1* had a transfer DNA (T-DNA) insertion in the 13th exon of the gene that resulted in embryonic lethality in the homozygotic state (Figure S1C). This agrees with prior reports indicating that NUP205 is essential for viability in *Arabidopsis thaliana* [11] and in *Saccharomyces cerevisiae* (NUP192) [12]. By contrast, a second allele, referred to as *nup205-3*, was viable. In *nup205-3*, the T-DNA insertion was toward the 3′ end of the gene, similar to the mutation in *eds4*. A full-length *NUP205* transcript could not be detected in the *nup205-3* mutant (Figure S1D), suggesting that this mutation might also result in a truncated version of NUP205.

To confirm that the clock phenotype of *eds4* was caused by the mutation in *NUP205* and to evaluate if the enhanced disease susceptibility phenotype *of eds4* was also caused by the same mutation, we assessed circadian and disease resistance phenotypes in the *nup205-3* mutant. Indeed, leaf movement assays demonstrated that the *nup205-3* allele had a longer circadian period than WT plants (Figure 2B), similar to that of *eds4* mutants. We also found comparable responses in *eds4* and *nup205-3* for light inhibition of hypocotyl growth and flowering time (Figures S1F–S1H). To evaluate disease susceptibility, leaves from five-week-old plants were pressure-infiltrated with *P. syringae* ES4326; bacterial growth assays at two days post-infection (2 d.p.i.) revealed a similar degree of susceptibility in *nup205-3* compared to *eds4* (Figure 2C), which was associated with reduced induction of *PR1* expression in response to *P. syringae* infection in both mutants (Figure S1E). Finally, we

performed classical genetic complementation tests by crossing *eds4* with *nup205-3* (Figure S1I) and found that the F1 progeny had a long circadian period and an enhanced disease susceptibility phenotype resembling the one observed in the parental mutant lines (Figures 2B and 2C). In contrast, WT circadian and disease susceptibility phenotypes were observed in *nup205-3* heterozygous plants resulting from a cross to WT plants, revealing the recessive nature of this mutation (Figures S1J and S1K), as previously reported for *eds4* [10]. Taken together, these results indicate that the circadian and disease susceptibility phenotypes of *eds4* are indeed caused by the mutation in *NUP205*.

NUP205 is one of the several nucleoporins that constitute the nuclear pore complex (NPC), which can be grouped into five different classes: transmembrane ring, core scaffold (inner ring and outer ring), cytoplasmic filaments, nuclear basket, and central phenylalanine-glycine repeat (FG) containing nups [13]. NUP205 is part of the inner ring sub-complex located in the central part of the nuclear pore together with NUP155, NUP188, NUP35, and the recently identified plant-specific nucleoporin CPR5 [13, 14]. Public data available from microarray experiments [15] show that the transcripts of most genes encoding NPC components present diurnal oscillations under 12-h light-dark cycles, and the expression of individual components of most sub-complexes is tightly synchronized (Figures S2A and S2C). Furthermore, the transcript levels of the inner ring components NUP205 and CPR5, but not those of other NUP components, showed consistent circadian expression profiles during the second and third days under continuous light conditions (Figures S2B and S2D). While there is emerging evidence that the composition of the NPC is flexible in other organisms [16], whether this is also true in plants remains to be fully determined.

Similar circadian defects (i.e., long-period phenotypes) have previously been reported for *nup* mutants that affect other NPC sub-complexes in *Arabidopsis thaliana* and in the fruit fly *Drosophila melanogaster* [17, 18]. Furthermore, other *Arabidopsis nup* mutants have been shown to display alterations in immune responses, photomorphogenic development, hormone signaling, and flowering time [14, 19]. Such pleiotropic effects could be simply due to general alterations in nucleocytoplasmic transport of most mRNAs and proteins. Alternatively, or in addition, some of the phenotypes displayed by *nup* mutants might be the direct consequence of alterations in the nucleocytoplasmic transport of specific subsets of mRNAs and/or proteins.

To start exploring these possibilities, we analyzed the transcriptome of 10-day-old seedlings grown under continuous white light (LL) from germination, without any prior exposure to light-dark or temperature cycles. Under this condition, circadian rhythms are strongly attenuated, and differences in mRNA levels are unlikely to result simply from differences in the phase of clock-regulated transcripts due to the period phenotype of the mutant. This analysis revealed a total of 492 differentially expressed genes (DEGs) in *eds4* (212 upregulated and 280 downregulated) compared to WT plants (Data S1). Gene ontology analysis of this group of genes showed significant enrichment in protein import categories among upregulated genes and mainly photosynthesis and responses to hormones and light stimulus categories among downregulated genes (Figure 3A; Data S1). Strikingly, more than half of the core clock genes (10 out of 17) and many clock ancillary genes (14 out of 44) were differentially expressed in the *eds4* mutant compared to WT plants (Figures 4A and S3A), a much greater proportion than expected by chance. Interestingly, most of the core clock genes with altered expression in *eds4* (8 out of 10 in total) were downregulated in the mutant.

Previous studies revealed that *nup* mutants have global defects in exporting mRNA from the nucleus, but whether nucleo-cytoplasmic partitioning of specific subsets of mRNAs is affected in these mutant plants is uncertain [11, 17, 20]. Here we used RNA sequencing (RNA-seq) to compare nuclear versus total relative abundance of individual mRNAs in a *nup* mutant and found a global mean of 20% enhancement in the genome-wide ratio of nuclear to total mRNA levels in *eds4* compared to WT seedlings (Figure 3C), which is similar to the approximately 25% increase in nuclear mRNA accumulation previously reported for the *nup160*, *nup85,* and *seh1* mutants [11]. As observed for DEGs, transcripts showing enhanced nuclear accumulation in the *eds4* mutant were also enriched in clock-related categories (Figure 3B). Indeed, the average nuclear to total ratio estimated for the mRNAs of core clock genes was 332% greater in *eds4* than in WT plants, an effect that was larger than in other functional categories (Figure 3C; Data S2). Together, these results show that specific subsets of mRNAs accumulate differentially in a *nup* mutant compared to WT plants, an effect that particularly impacts the mRNAs of circadian clock genes.

Bacterial infection, or salicylic acid (SA) treatment, has been shown to affect the expression of core clock genes several hours after treatment [2, 3], but if and how bacterial infection triggers more rapid changes in core clock gene expression has not been evaluated. Here we analyzed publicly available RNA-seq data from *Arabidopsis* plants infected with a virulent strain of *Pseudomonas syringae* pathovar (pv) tomato DC3000 [21] and identified a massive enrichment in clock genes among those differentially expressed as early as one h post-infection (1 h.p.i.) (Figures 4A and S4A; Data S3).

The plant circadian clock depends on a complex gene network in which many repressors and some activators mutually regulate each other's expression. CIRCADIAN CLOCK ASSOCIATED 1 (CCA1) and LATE ELONGATED HYPOCOTYL (LHY) show peak expression in the morning and repress the expression of the *PSEUDORESPONSE REGULATOR* (*PRR*) genes *PRR9*, *PRR7*, *PRR5*, and *PRR1* also known as *TIMING OF CAB EXPRESSION 1* (*TOC1*), whose levels peak from midday to late afternoon and feed back to repress *CCA1* and *LHY* expression throughout the day. In the evening, LUX ARRHYTHMO (LUX), EARLY FLOWERING 4 (ELF4), and ELF3 form the evening complex (EC), which represses the expression of *PRR9* and *LUX* itself. The clock gene network also involves transcriptional activators such as members of the REVEILLE (RVE) and NIGHT LIGHT INDUCIBLE AND CLOCK-REGULATED (LNK) families, which interact to enhance the expression of afternoon and evening genes such as *PRR5*, *TOC1,* and *ELF4*. We observed that bacterial infection triggered a significant reconfiguration of the core clock gene network, resulting in the downregulation of morning clock genes, including

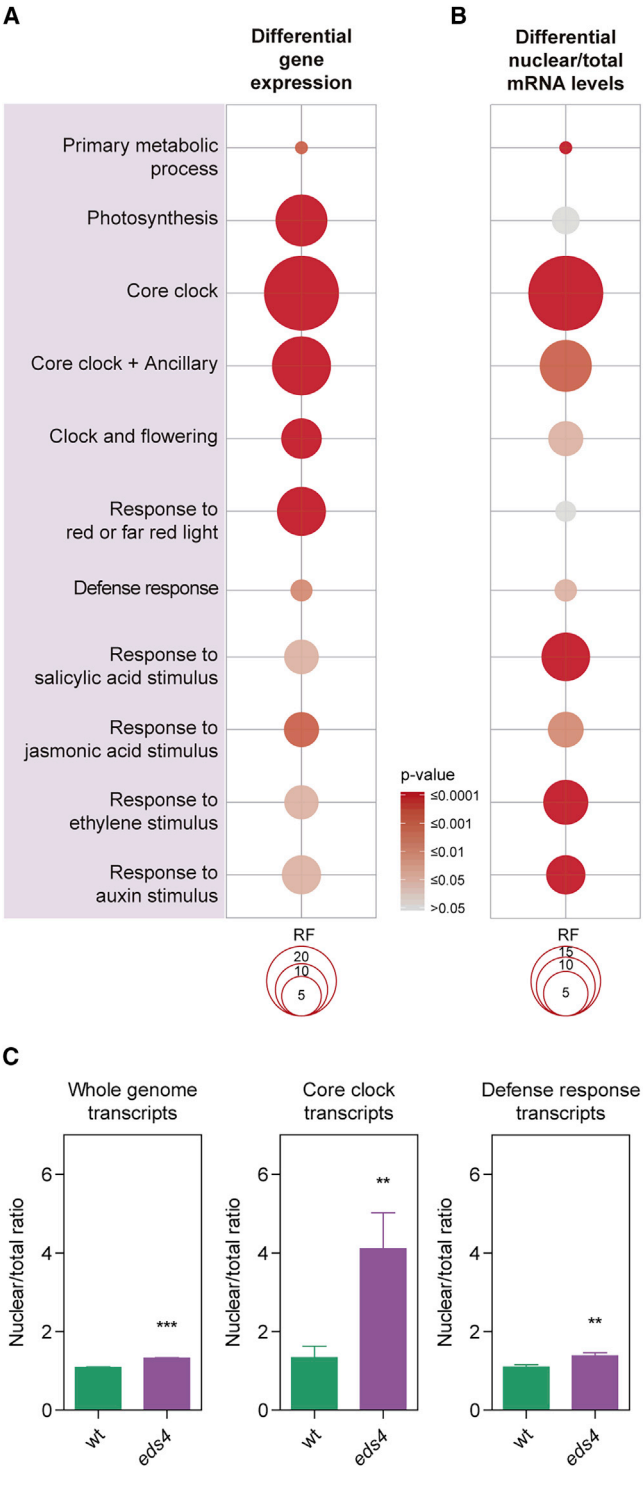

Figure 3. EDS4 Impact on Gene Expression and Nuclear to Total Relative mRNA Levels

(A and B) Representation factor (RF) of selected gene ontologies and functional categories among genes with differential expression (A) and gene transcripts with differential nuclear to total relative mRNA levels (B) in the *eds4* mutant compared to WT plants under continuous LL. RF significance (p value) is shown in a red intensity scale and was assessed using a hypergeometric test.

(C) Abundance ratio between nucleus-located transcripts and nucleus-plus-cytoplasm-located transcripts (total) for the whole genome, core clock genes, and defense response genes. Error bars indicate SEM. ns = non-significant; $^{**}p < 0.01$; $^{***}p < 0.001$ (Student's t test). See also Data S1 and S2.

the four members of the *LNK* gene family, which we validated by quantitative PCR (qPCR) (Figures 4B–4C and S4A). This transcriptomic reconfiguration resembled that observed in *eds4* mutants under control conditions (i.e., in *eds4* plants not exposed to pathogens) (Figures 4B and S4B).

To assess the role of EDS4 on the effect of pathogen infection over clock gene expression, we infected 5-week-old WT and *eds4* plants grown under SD conditions with either a mock solution (10mM $MgSO_4$) or a bacterial suspension of *P. syringae* DC3000 at dawn. Measurements of clock gene expression by qPCR at 1 h.p.i. confirmed that the entire *LNK* gene family was downregulated (Figure 4C). The effect of bacterial infection on the expression of most of the *LNK* clock genes was attenuated in *eds4* mutant plants, which could be due in part to the already lower level of expression of these genes in *eds4* compared to the WT (Figure 4C). Whether bacterial infection alters the expression of core clock genes by affecting EDS4 levels and/or activity is unknown, but CPR5, one of the other members of NUP205 sub-complex, was shown to undergo conformational changes upon activation by immunoreceptors, releasing effector-triggered immunity (ETI) signaling components and at the same time reconfiguring the NPC selective barrier [14]. Whether bacterial effectors alter the activity of some NPC components in our infection assays, which do not trigger ETI, remains to be determined.

While alterations in disease resistance have been reported for plants with altered expression levels of clock genes that act as repressors [1, 4], it is not known whether transcriptional activators, such as the LNKs, modulate host-pathogen interactions. We observed that *lnk1lnk2lnk3lnk4* quadruple mutants (*lnkQ*) [22], which also present a long-period phenotype in leaf movement assays (Figure 4D), were much more susceptible to *Pseudomonas syringae* DC3000 infection than WT plants (Figure 4E). This effect was also present, but to a slightly lower extent, in *lnk1lnk2* (*lnk1/2*) double mutants [23] (Figure S4C). Interestingly, a significant effect of the *LNK* genes on susceptibility was observed regardless of the time of infection (Figure 4E). Furthermore, the enhancement in disease susceptibility of the *lnkQ* mutant was similar to that of *eds4*, despite the larger effect of the former on period length. These observations, taken together, suggest that the contribution of EDS4 and the LNKs to plant defense against bacterial infection may not result from their effect on clock period. Alternatively, we cannot exclude the possibility that these genes control immunity through partially different mechanisms. Although the precise mechanisms through which EDS4 and the LNKs modulate disease susceptibility remains to be determined, it is possible that clock genes, such as the LNKs, have a direct and specific role in pathogen resistance, and that the *eds4* susceptibility phenotype results, at least to some extent, from the alteration of this direct function of the LNKs. In favor of this possibility we see a larger-than-expected-by-chance overlap between genes whose expression is altered in *eds4* and in *lnk1/2* mutants

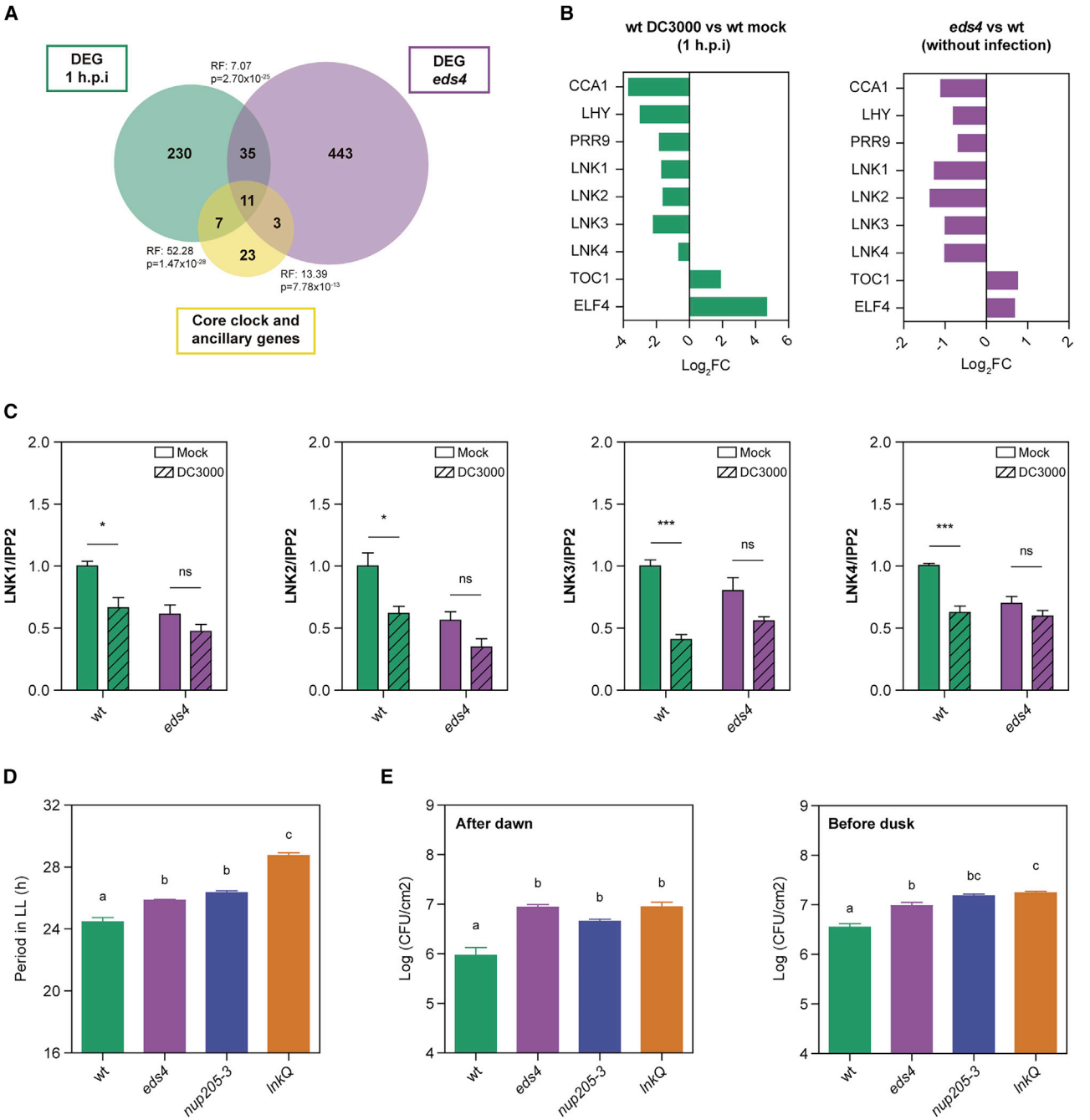

Figure 4. The *LNK* Gene Family Plays a Key Role Modulating Plant-Pathogen Interactions

(A) Overlap between differentially expressed genes (DEGs) in *eds4* mutants grown in continuous LL under non-infective conditions (DEG *eds4*), DEGs in publicly available RNA-seq data of *P. syringae* DC3000 infected WT plants grown in SD conditions 1 h.p.i. in the morning (DEG 1 h.p.i.), and core clock and ancillary genes. RF significance was assessed using a hypergeometric test ($p \leq 0.05$). See also Figure S3.

(B) Differential expression profile of core clock genes in publicly available RNA-seq data of *P. syringae* DC3000-infected WT plants (DEG 1 h.p.i.) versus mock-treated plants grown in SD conditions (left) and in the *eds4* mutant compared to WT plants under non-infected normal conditions in LL (right). See also Figures S4A–S4B; Data S1 and S3.

(C) Expression levels of *LNK1*, *LNK2*, *LNK3*, and *LNK4* measured by qRT-PCR. The analysis was conducted in WT and *eds4* plants grown under an SD photoperiod 1 h post-infiltration (at ZT = 2) with either a mock solution (10 mM $MgSO_4$) or a bacterial suspension (DC3000; OD_{600} = 0.002) (n = 6 biological replicates). Results were calculated relative to IPP2 transcript levels and indicate mean values relative to mock-treated WT plants in 2 independent experiments. Error bars indicate SEM, ns: non-significant, *$p < 0.05$, ***$p < 0.001$ (Two-way ANOVA followed by Tukey's multi-comparison test; non-significant interaction between genotype and treatment for the *LNK1* and *LNK2* genes, significant interaction for the *LNK3* and *LNK4* genes; $p < 0.05$).

(legend continued on next page)

(Figure S4D). While many of the overlapping genes are clock genes, some are proper defense genes, such as *ACD6*, whose expression was reduced in both mutant types (Data S1).

In summary, we found that an early event following bacterial infection in plants includes a very rapid reconfiguration of the core clock gene expression network, which in turn controls immune responses as part of its outputs. This transcriptional reprogramming requires to some extent a functional NPC, which is regulated, at least in part, by the clock itself (Figure S4E). The disruption of the clock gene network, which includes the downregulation of the *LNK* gene family, enhances bacterial growth and disease susceptibility.

STAR★METHODS

Detailed methods are provided in the online version of this paper and include the following:

- KEY RESOURCES TABLE
- LEAD CONTACT AND MATERIALS AVAILABILITY
- EXPERIMENTAL MODEL AND SUBJECT DETAILS
  - Plant material
  - Plant Growth conditions
  - *Pseudomonas syringae* culture conditions
  - Accession numbers
- METHOD DETAILS
  - Circadian leaf movement analysis
  - Hypocotyl length measurements
  - Flowering time analysis
  - Bioluminescence assays
  - Whole-genome resequencing of Col-0 and *eds4*
  - Mapping by sequencing
  - SNP validation
  - Assessing embryonic lethality in *nup205-1*
  - NUP205 expression in wt, *eds4* and *nup205-3* backgrounds
  - Bacterial growth assays
  - Growth conditions and protocol used for cDNA library preparation and high-throughput sequencing
  - Processing of RNA sequencing reads
  - Differential gene expression analysis
  - *In silico* validation of nuclei enrichment in nuclear samples
  - Differential nuclear to total transcripts' accumulation
  - Functional category enrichment analysis
  - Estimation of nuclear to total ratio
  - Differentially expressed genes 1 h post infection
  - Quantitative PCR analysis of circadian clock gene expression at 1 h.p.i
  - Quantitative PCR analysis of circadian clock gene expression in SD
- QUANTIFICATION AND STATISTICAL ANALYSIS
- DATA AND CODE AVAILABILITY

SUPPLEMENTAL INFORMATION

Supplemental Information can be found online at https://doi.org/10.1016/j.cub.2020.02.058.

ACKNOWLEDGMENTS

We thank J. Hildebrandt, D. Lundberg, E. Symeonidi, and the Weigel laboratory at the Max Planck Institute for Developmental Biology in Tübingen for technical assistance in the DNA sequencing; J. Mateos and S. Mora-García for helpful discussion on the project; and P. Cerdán for suggestions for the mapping process. This work was supported by grants from the Agencia Nacional de Promoción Científica y Tecnológica of Argentina (to M.J.Y.).

AUTHOR CONTRIBUTIONS

M.J.d.L., C.E.H., D.A.C., and A.F.S. performed the experiments and statistical analysis. A.R. obtained LNK quadruple mutant. C.E.H. constructed the complementary DNA (cDNA) libraries and performed the bioinformatic analysis of the RNAseq data. M.V. performed the RNA-seq protocols. H.S. executed and K.S. supervised SHOREmapping. N.G.B. performed the nuclear and total RNA extraction. M.J.d.L. and M.J.Y. wrote the paper. M.J.Y. supervised the project. All authors discussed the results and commented on the manuscript.

DECLARATION OF INTERESTS

The authors declare no competing interests.

Received: September 23, 2019
Revised: January 22, 2020
Accepted: February 20, 2020
Published: March 26, 2020

REFERENCES

1. Lu, H., McClung, C.R., and Zhang, C. (2017). Tick Tock: Circadian Regulation of Plant Innate Immunity. Annu. Rev. Phytopathol. *55*, 287–311.
2. Li, Z., Bonaldi, K., Uribe, F., and Pruneda-Paz, J.L. (2018). A Localized Pseudomonas syringae Infection Triggers Systemic Clock Responses in Arabidopsis. Curr. Biol. *28*, 630–639e4.
3. Zhou, M., Wang, W., Karapetyan, S., Mwimba, M., Marqués, J., Buchler, N.E., and Dong, X. (2015). Redox rhythm reinforces the circadian clock to gate immune response. Nature *523*, 472–476.
4. Zhang, C., Gao, M., Seitz, N.C., Angel, W., Hallworth, A., Wiratan, L., Darwish, O., Alkharouf, N., Dawit, T., Lin, D., et al. (2019). LUX ARRHYTHMO mediates crosstalk between the circadian clock and defense in Arabidopsis. Nat. Commun. *10*, 2543.
5. Jirage, D., Tootle, T.L., Reuber, T.L., Frost, L.N., Feys, B.J., Parker, J.E., Ausubel, F.M., and Glazebrook, J. (1999). Arabidopsis thaliana PAD4 encodes a lipase-like gene that is important for salicylic acid signaling. Proc. Natl. Acad. Sci. USA *96*, 13583–13588.
6. Century, K.S., Holub, E.B., and Staskawicz, B.J. (1995). NDR1, a locus of Arabidopsis thaliana that is required for disease resistance to both a bacterial and a fungal pathogen. Proc. Natl. Acad. Sci. USA *92*, 6597–6601.
7. Cao, H., Bowling, S.A., Gordon, A.S., and Dong, X. (1994). Characterization of an Arabidopsis Mutant That Is Nonresponsive to Inducers of Systemic Acquired Resistance. Plant Cell *6*, 1583–1592.
8. Glazebrook, J., Rogers, E.E., and Ausubel, F.M. (1996). Isolation of Arabidopsis mutants with enhanced disease susceptibility by direct screening. Genetics *143*, 973–982.

(D) Period length of circadian rhythms associated with leaf movement (n = 6 plants) in WT, *eds4, nup205-3*, and *lnk1/lnk2/lnk3/lnk4* quadruple mutant (*lnkQ*) 10-day-old plants.

(E) Bacterial growth assessed at 2 d.p.i. in 5- to 6-week-old plants grown in SD conditions and infiltrated with DC3000 after dawn (ZT = 2) or before dusk (ZT = 8) (n = 8 plants). See also Figure S4C. Error bars indicate SEM. Different letters indicate significant difference among genotypes. $p < 0.05$ (one-way ANOVA followed by Tukey's multi-comparison test). These experiments were repeated at least three times with similar results.

9. Hayama, R., and Coupland, G. (2004). The molecular basis of diversity in the photoperiodic flowering responses of Arabidopsis and rice. Plant Physiol. *135*, 677–684.
10. Gupta, V., Willits, M.G., and Glazebrook, J. (2000). Arabidopsis thaliana EDS4 contributes to salicylic acid (SA)-dependent expression of defense responses: evidence for inhibition of jasmonic acid signaling by SA. Mol. Plant Microbe Interact. *13*, 503–511.
11. Parry, G. (2014). Components of the Arabidopsis nuclear pore complex play multiple diverse roles in control of plant growth. J. Exp. Bot. *65*, 6057–6067.
12. Kosova, B., Panté, N., Rollenhagen, C., and Hurt, E. (1999). Nup192p is a conserved nucleoporin with a preferential location at the inner site of the nuclear membrane. J. Biol. Chem. *274*, 22646–22651.
13. Tamura, K., and Hara-Nishimura, I. (2013). The molecular architecture of the plant nuclear pore complex. J. Exp. Bot. *64*, 823–832.
14. Gu, Y., Zebell, S.G., Liang, Z., Wang, S., Kang, B.-H., and Dong, X. (2016). Nuclear Pore Permeabilization Is a Convergent Signaling Event in Effector-Triggered Immunity. Cell *166*, 1526–1538e11.
15. Mockler, T.C., Michael, T.P., Priest, H.D., Shen, R., Sullivan, C.M., Givan, S.A., McEntee, C., Kay, S.A., and Chory, J. (2007). The DIURNAL project: DIURNAL and circadian expression profiling, model-based pattern matching, and promoter analysis. Cold Spring Harb. Symp. Quant. Biol. *72*, 353–363.
16. Knockenhauer, K.E., and Schwartz, T.U. (2016). The Nuclear Pore Complex as a Flexible and Dynamic Gate. Cell *164*, 1162–1171.
17. MacGregor, D.R., Gould, P., Foreman, J., Griffiths, J., Bird, S., Page, R., Stewart, K., Steel, G., Young, J., Paszkiewicz, K., et al. (2013). HIGH EXPRESSION OF OSMOTICALLY RESPONSIVE GENES1 is required for circadian periodicity through the promotion of nucleo-cytoplasmic mRNA export in Arabidopsis. Plant Cell *25*, 4391–4404.
18. Szabó, Á., Papin, C., Cornu, D., Chélot, E., Lipinszki, Z., Udvardy, A., Redeker, V., Mayor, U., and Rouyer, F. (2018). Ubiquitylation Dynamics of the Clock Cell Proteome and TIMELESS during a Circadian Cycle. Cell Rep. *23*, 2273–2282.
19. Parry, G. (2013). Assessing the function of the plant nuclear pore complex and the search for specificity. J. Exp. Bot. *64*, 833–845.
20. Wiermer, M., Cheng, Y.T., Imkampe, J., Li, M., Wang, D., Lipka, V., and Li, X. (2012). Putative members of the Arabidopsis Nup107-160 nuclear pore sub-complex contribute to pathogen defense. Plant J. *70*, 796–808.
21. Howard, B.E., Hu, Q., Babaoglu, A.C., Chandra, M., Borghi, M., Tan, X., He, L., Winter-Sederoff, H., Gassmann, W., Veronese, P., and Heber, S. (2013). High-throughput RNA sequencing of pseudomonas-infected Arabidopsis reveals hidden transcriptome complexity and novel splice variants. PLoS ONE *8*, e74183.
22. de Leone, M.J., Hernando, C.E., Romanowski, A., García-Hourquet, M., Careno, D., Casal, J., Rugnone, M., Mora-García, S., and Yanovsky, M.J. (2018). The LNK Gene Family: At the Crossroad between Light Signaling and the Circadian Clock. Genes (Basel) *10*, E2.
23. Rugnone, M.L., Faigón Soverna, A., Sanchez, S.E., Schlaen, R.G., Hernando, C.E., Seymour, D.K., Mancini, E., Chernomoretz, A., Weigel, D., Más, P., and Yanovsky, M.J. (2013). LNK genes integrate light and clock signaling networks at the core of the Arabidopsis oscillator. Proc. Natl. Acad. Sci. USA *110*, 12120–12125.
24. Dong, X., Mindrinos, M., Davis, K.R., and Ausubel, F.M. (1991). Induction of Arabidopsis defense genes by virulent and avirulent Pseudomonas syringae strains and by a cloned avirulence gene. Plant Cell *3*, 61–72.
25. Cuppels, D.A. (1986). Generation and Characterization of Tn5 Insertion Mutations in Pseudomonas syringae pv. tomato. Appl. Environ. Microbiol. *51*, 323–327.
26. Fan, J., Crooks, C., and Lamb, C. (2008). High-throughput quantitative luminescence assay of the growth in planta of Pseudomonas syringae chromosomally tagged with Photorhabdus luminescens luxCDABE. Plant J. *53*, 393–399.
27. Plautz, J.D., Straume, M., Stanewsky, R., Jamison, C.F., Brandes, C., Dowse, H.B., Hall, J.C., and Kay, S.A. (1997). Quantitative analysis of Drosophila period gene transcription in living animals. J. Biol. Rhythms *12*, 204–217.
28. Schneider, C.A., Rasband, W.S., and Eliceiri, K.W. (2012). NIH Image to ImageJ: 25 years of image analysis. Nat. Methods *9*, 671–675.
29. Sun, H., and Schneeberger, K. (2015). SHOREmap v3.0: fast and accurate identification of causal mutations from forward genetic screens. Methods Mol. Biol. *1284*, 381–395.
30. Neff, M.M., Turk, E., and Kalishman, M. (2002). Web-based primer design for single nucleotide polymorphism analysis. Trends Genet. *18*, 613–615.
31. Trapnell, C., Pachter, L., and Salzberg, S.L. (2009). TopHat: discovering splice junctions with RNA-Seq. Bioinformatics *25*, 1105–1111.
32. Robinson, M.D., McCarthy, D.J., and Smyth, G.K. (2010). edgeR: a Bioconductor package for differential expression analysis of digital gene expression data. Bioinformatics *26*, 139–140.
33. Hulsen, T., de Vlieg, J., and Alkema, W. (2008). BioVenn - a web application for the comparison and visualization of biological lists using area-proportional Venn diagrams. BMC Genomics *9*, 488.
34. Koornneef, M., Hanhart, C.J., and van der Veen, J.H. (1991). A genetic and physiological analysis of late flowering mutants in Arabidopsis thaliana. Mol. Gen. Genet. *229*, 57–66.
35. Clough, S.J., and Bent, A.F. (1998). Floral dip: a simplified method for Agrobacterium-mediated transformation of Arabidopsis thaliana. Plant J. *16*, 735–743.
36. Neff, M.M., Neff, J.D., Chory, J., and Pepper, A.E. (1998). dCAPS, a simple technique for the genetic analysis of single nucleotide polymorphisms: experimental applications in Arabidopsis thaliana genetics. Plant J. *14*, 387–392.
37. Weigel, D., and Glazebrook, J. (2002). Arabidopsis: A Laboratory Manual (Cold Spring Harbor Laboratory Press).
38. Bologna, N.G., Iselin, R., Abriata, L.A., Sarazin, A., Pumplin, N., Jay, F., Grentzinger, T., Dal Peraro, M., and Voinnet, O. (2018). Nucleo-cytosolic Shuttling of ARGONAUTE1 Prompts a Revised Model of the Plant MicroRNA Pathway. Mol. Cell *69*, 709–719e5.
39. Lamesch, P., Berardini, T.Z., Li, D., Swarbreck, D., Wilks, C., Sasidharan, R., Muller, R., Dreher, K., Alexander, D.L., Garcia-Hernandez, M., et al. (2012). The Arabidopsis Information Resource (TAIR): improved gene annotation and new tools. Nucleic Acids Res. *40*, D1202–D1210.
40. Benjamini, Y., and Hochberg, Y. (1995). Controlling the False Discovery Rate: A Practical and Powerful Approach to Multiple Testing. J. R. Statist. Soc. B. *57*, 289–300.
41. Katari, M.S., Nowicki, S.D., Aceituno, F.F., Nero, D., Kelfer, J., Thompson, L.P., Cabello, J.M., Davidson, R.S., Goldberg, A.P., Shasha, D.E., et al. (2010). VirtualPlant: a software platform to support systems biology research. Plant Physiol. *152*, 500–515.
42. Schmittgen, T.D., and Livak, K.J. (2008). Analyzing real-time PCR data by the comparative C(T) method. Nat. Protoc. *3*, 1101–1108.

STAR★METHODS

KEY RESOURCES TABLE

REAGENT or RESOURCE	SOURCE	IDENTIFIER
Bacterial and Virus Strains		
Pseudomonas syringae pv. maculicolia ES4326	[24]	N/A
Pseudomonas syringae pv. tomato DC3000	[25]	N/A
Pseudomonas syringae pv. ES4326 luxCDABE-tagged	[26]	N/A
Agrobacterium tumefaciens GV3101 strain	GoldBio	Cat#: CC-207-A
Chemicals, Peptides, and Recombinant Proteins		
Murashige & Skoog Medium	Duchefa Biochemie	Cat#: M0221
Bacteriological Agar	Britania	Cat#: B0101406
Sucrose	Cicarelli	Cat#: 841214
Rifampicin	Duchefa Biochemie	Cat#: R0146
D-Luciferin Firefly, potassium salt	Duchefa Biochemie	Cat#: L1349
Taq DNA Polymerase, recombinant	Thermo Fisher Scientific	Cat#: 10342020
Agarose SPI	Duchefa Biochemie	Cat#: A1203
TRIZol Reagent	Thermo Fisher Scientific	Cat#: 15596026
Super Script II Reverse Transcriptase	Thermo Fisher Scientific	Cat#: 18064022
FastStart Universal SYBR Green Master	Roche	Cat#: 04913914001
RQ1 RNase-Free DNase	Promega	Cat#: M6101
Critical Commercial Assays		
Plant DNeasy Kit	QIAGEN	Cat#: 69104
Truseq Nano DNA Library Prep Kit	Illumina	Cat#: 20015964
Agilent DNA1000 Kit	Agilent Technologies	Cat#: 5067-1504
RNeasy Plant Mini Kit	QIAGEN	Cat#: 74904
TruSeq RNA Library Prep Kit v2	Illumina	Cat#: RS-122-2001
Deposited Data		
Whole genome sequencing datasets	This paper	SRA: PRJNA493644 https://www.ncbi.nlm.nih.gov/sra/PRJNA493644
RNA high-throughput sequencing data	This paper	GEO: GSE120757 https://www.ncbi.nlm.nih.gov/geo/query/acc.cgi?acc=GSE120757
RNA-seq data of P. syringae DC3000 infected WT plants 1 h.p.i.	[21] datasets	https://doi.org/10.1371/journal.pone.0074183
Arabidopsis thaliana TAIR10 genome	The *Arabidopsis* Information Resource	https://www.arabidopsis.org/index.jsp
Experimental Models: Organisms/Strains		
Arabidopsis thaliana Col-0	ABRC	Stock#: CS849018
Arabidopsis thaliana eds4-1	NASC	Stock#: CS3799
Arabidopsis thaliana npr1-1	NASC	Stock#: CS3726
Arabidopsis thaliana ndr1-1	NASC	Stock#: CS68768
Arabidopsis thaliana pad4-1	NASC	Stock#: CS3806
Arabidopsis thaliana nup205-1	NASC	Stock#: SALK_055559
Arabidopsis thaliana nup205-3	NASC	Stock#: GK_155G03
Arabidopsis thaliana eds4 pCCA1::LUC	This study	N/A
Arabidopsis thaliana eds4 pTOC1::LUC	This study	N/A
Arabidopsis thaliana lnk1-2	[23]	N/A
Arabidopsis thaliana lnk3-4	[22]	N/A
Arabidopsis thaliana lnkQ	[22]	N/A

(*Continued on next page*)

Continued		
REAGENT or RESOURCE	SOURCE	IDENTIFIER
Oligonucleotides		
See Table S2		N/A
Recombinant DNA		
CCA1:LUC plasmid	S. Harmer Lab	http://harmerlab.plantclock.org/
TOC1:LUC plasmid	S. Harmer Lab	http://harmerlab.plantclock.org/
Software and Algorithms		
Brass 3.0 software (Biological Rhythms Analysis Software System)	A. Millar Lab	https://www.ed.ac.uk/profile/andrew-millar
fast Fourier transform-non-linear least-squares (FFT-NLLS) algorithm	[27]	N/A
ImageJ	[28]	https://imagej.nih.gov/ij/
GraphPad Prism version 6	GraphPad software	https://www.graphpad.com/
Mikrowin 2000 (version 4.29)	Labsis	https://labsis.de/index.php
SHOREmap 3.0 computational tool kit	[29]	http://bioinfo.mpipz.mpg.de/shoremap/
dCAPS finder 2.0	[30]	http://helix.wustl.edu/dcaps/
TopHat v2.1.1	[31]	http://ccb.jhu.edu/software/tophat/index.shtml
edgeR package version 3.4.2	[32]	http://bioconductor.org/packages/release/bioc/html/edgeR.html
BioVenn	[33]	http://www.biovenn.nl/
BioMaps	Virtual Plant	http://virtualplant.bio.nyu.edu/cgi-bin/vpweb
Other		
Growmix multipro soil	Terrafertil	N/A
Microplate luminometer	Berthold Technologies	Model#: LB-960
Agilent 2100 Bioanalyzer	Agilent Technologies	N/A
Sequencing systems	Illumina	HiSeq1500 and HiSeq2000

LEAD CONTACT AND MATERIALS AVAILABILITY

Further information and requests for protocols, bioinformatic resources, *Arabidopsis thaliana* mutant seeds, bacterial strains and recombinant DNA constructs should be directed to and will be fulfilled by the Lead Contact, Marcelo J. Yanovsky (myanovsky@leloir.org.ar).

EXPERIMENTAL MODEL AND SUBJECT DETAILS

Plant material

All the mutants used in this study were in a Columbia (Col-0) accession background of *Arabidopsis thaliana*. *pad4-1* (CS3806), *ndr1-1* (CS68768), *npr1-1* (CS3726), *nup205-1* (SALK_055559), and *nup205-3* (GK_155G03) mutant seeds were obtained from the Nottingham *Arabidopsis* Stock Centre (NASC). *lnk1-1* (SALK_024353), *lnk2-1* (GK_484F07), *lnk3-1* (SALK_085551C), *lnk4-1* (GK_846C06) were acquired from the *Arabidopsis* Biological Research Center (ABRC) T-DNA insertion collection and the double and quadruple mutants were obtained by crossing single mutants. The photoreceptor mutants used in this study were *phyB-9*, and *cry1-b104;cry2-1*.

Plant Growth conditions

Plants were grown on soil or Murashige and Skoog medium containing 0.8% (w/v) agar (supplemented or not with 1% (w/v) sucrose, as specified in each experiment) at 22°C under long days (LD; 16-h light/8-h dark cycles; 80 μmol.m^{-2}.s^{-1} of white light), short days (SD; 8-h light/16-h dark cycles; 140 μmol.m^{-2}.s^{-1} of white light), or continuous light (LL; 50 μmol$\cdot$m$^{-2}\cdot$s^{-1} of white light), depending on the experiment.

Pseudomonas syringae culture conditions

Pseudomonas syringae pv. maculicolia ES4326 [24], *Pseudomonas syringae* pv. tomato DC3000 [25] or luxCDABE-tagged ES4326 [26] strains were grown at 28°C with King's B medium (20 g protease peptone, 1.5 g K2HPO4, 6.09 mL 1 M MgSO4, and 10 g glycerol per liter) supplemented with rifampicin (100mg/L) and/or kanamycin (50mg/L) for selection.

Accession numbers

Gene models in this article can be found in The *Arabidopsis* Information Resource (TAIR) (https://www.arabidopsis.org/) with the following accession numbers: PAD4, At3g52430; NDR1, At3g20600; NPR1, At1g64280; NUP205, At5g51200; PR1, At2g14610; CCA1, At2g46830; LHY, At1g01060; PPR9, At2g46790; LNK1, At5g64170; LNK2, At3g54500; LNK3, At3g12320; LNK4, At5g06980.

METHOD DETAILS

Circadian leaf movement analysis

For leaf movement analysis, plants were grown under 16-h light/8-h dark (LD) cycles and transferred to continuous 20 μmol.m^{-2}.s^{-1} white fluorescent light at 22°C, and the movement of the first pair of leaves was recorded every 2 h for 5-6 days using digital cameras. The leaf angle formed by the tip of the petiole and the point of insertion of the first pair of true leaves in the stem was determined using ImageJ software [28]. Period estimates were calculated with Brass 3.0 software (Biological Rhythms Analysis Software System, available from https://www.ed.ac.uk/profile/andrew-millar) and analyzed with Fast Fourier Transform-Non-Linear Least-squares (FFT-NLLS) suite of programs, as described previously [27].

Hypocotyl length measurements

For hypocotyl length measurements seedlings were grown on 0.8% (m/v) agar without sucrose in complete darkness, continuous red light (0.01 to 100 μmol.m^{-2}.s^{-1}), continuous blue light (0.1 to 10 μmol.m^{-2}.s^{-1}), continuous white light (LL) and cycling white light in SD and LD. The final length of the hypocotyls was measured after 4 d. Light effects on hypocotyl elongation under different wavelengths (red and blue) were calculated by normalizing hypocotyl length under each light regime relative to hypocotyl length of the same genotype under constant dark conditions in order to dissociate growth defects from light-sensing alterations; n = 6 replicates of 10 seedlings each. The *phyb* null mutant for the red light photoreceptor Phytochrome B, and the *cry1/2* double mutant for the blue light photoreceptors Cryptochrome 1 and Cryptochrome 2 were used as hyposensitive controls.

Flowering time analysis

For flowering time experiments, the plants were grown on soil at 22°C under long days (LD; 16-h light/8-h dark cycles; 80 μmol.m^{-2}.s^{-1} of white light) or short days (SD;8-h light/16-h dark cycles; 140 μmol.m^{-2}.s^{-1} of white light) depending on the experiment. Flowering time was estimated by counting the number of rosette leaves at the time of bolting as proposed by Koornneef et al. [34].

Bioluminescence assays

For bioluminescence assays transgenic wt and *eds4* lines were obtained by transformation with bioluminescent reporter constructs carrying the firefly luciferase (LUC) gene under the control of core clock genes CCA1 and TOC1 promoters (pCCA1::LUC and pTOC1::LUC respectively) using the floral dip method [35]. Seedlings were grown directly on Murashige and Skoog 0.8% (w/v) agar supplemented with 1% (w/v) sucrose in a 96-well plate. One seed was placed per well and then the seedlings were entrained under a 16-h light/8-h dark cycle. After 7 days, the entire plate was transferred to constant light conditions and placed in a microplate luminometer LB-960 (Berthold Technologies) to measure bioluminescence emitted by each seedling every hour. After 5–6 days, data were obtained using Mikrowin 2000 (version 4.29). Period estimates were calculated with Brass 3.0 software (Biological Rhythms Analysis Software System; https://www.ed.ac.uk/profile/andrew-millar) and analyzed using FFT-NLLS suite of programs, as described previously [27].

Whole-genome resequencing of Col-0 and *eds4*

A total of four samples were prepared: one single *eds4* plant and one single Col-0 plant, as well as one pool of 60 *eds4* plants and one pool of 60 Col-0 plants. DNA was isolated using a Plant DNeasy Kit (QIAGEN), following the manufacturer's protocols, and then processed according to the Truseq Nano DNA Library Prep Kit and protocol (Illumina). Fragmentation was performed by Covaris ultrasonication and an enrichment step of 7 cycles of PCR was performed. Library validation included size and purity assessment with the Agilent 2100 Bioanalyzer and the Agilent DNA1000 Kit (Agilent Technologies). DNA libraries were pair-end sequenced with an Illumina HiSeq2000 in Detlef Weigel's Lab at the Max Planck Institute for Developmental Biology (Tübingen, Germany). Sequencing data have been uploaded to the Sequence Read Archive (SRA) and are available under accession number PRJNA493644.

Mapping by sequencing

The resequencing data obtained from pooled and single *eds4* and Col-0 genomes were analyzed using SHOREmap 3.0 computational tool kit [29]. A list of the 19 candidate SNPs found in the *eds4* mutant genome can be found in Data S1.

SNP validation

To validate the differential SNPs found between *eds4* and Col-0 a multiple dCAPS analysis [36] was performed. PCR primers for dCAPS were designed using dCAPS finder 2.0 [30]. A standard PCR protocol was used to amplify products from *eds4* and Col-0 and the PCR products were digested and separated on a 3% (w/v) agarose gel. Summary of primers and restriction enzymes used for each SNP's validation is available upon request.

Assessing embryonic lethality in *nup205-1*

Fully developed Col-0 and *nup205-1* siliques were fixed in an ethanol/acetic acid (2:1) mixture and the clarified in a chloral hydrate/glycerol/water (8:1:2) mixture as previously described [37]. Samples were then mounted, and aborted seeds counted in each silique (n = 10 biological replicates).

NUP205 expression in wt, *eds4* and *nup205-3* backgrounds

Plants were grown in SD conditions for 5-6 weeks. Tissue was harvested and total RNA was extracted using TRIzol reagent (Invitrogen) according to the manufacturer's protocol. One microgram of RNA was treated with RQ1 RNase-Free DNase (Promega) and subjected to retro transcription with Super Script II Reverse Transcriptase (Thermo Fisher Scientific) and oligo-dT, according to manufacturer's instructions. A standard PCR protocol was used to amplify products from *eds4* and Col-0 cDNAs. The PCR products were then separated on a 1% (w/v) agarose gel. Primers sequences used are summarized in Table S1.

Bacterial growth assays

Freshly cultured bacteria were collected and re-suspended to a final concentration of OD_{600} = 0.0002 in 10 mM $MgSO_4$. The bacterial solution was then pressured-infiltrated with a 1 mL needleless syringe into the abaxial side of the eighth to tenth leaves of 5- to 6-week-old plant grown under SD conditions (at ZT = 2 or ZT = 8, depending on the experiment). Bacterial growth assays were performed at 48 h post infection (h.p.i). Leaves were surface washed in sterile water before carrying out bacterial-load determination.

For the quantification by counting of bacterial colonies in plate assays, a disc was punched from each leaf and then the three discs corresponding to each plant were placed in 750 μL of 10 mM $MgCl_2$ and crushed to release the bacteria. The resulting solution was serially diluted, and spot plated on KB plates containing the corresponding antibiotics. The plates were incubated at 28°C for 48 h prior to counting of the colonies and performing a log-transformed bacterial growth statistical analysis.

For the quantification by measurement of bioluminescence using the luxCDABE-tagged *Pseudomonas syringae pv*. ES4326 [26] strains, a disc was punched from each leaf and then the three discs where separately placed in 200 μL of 10 mM $MgCl_2$ in a multiwall plate. The bioluminescence emitted by each disk was the measured in a microplate luminometer LB-960 (Berthold Technologies). An average luminescence value was estimated for each plant, which is indicated relative to the average value obtained for wt Col-0 plants.

Growth conditions and protocol used for cDNA library preparation and high-throughput sequencing

For the differential gene expression analysis, Col-0 and *eds4* seeds were sown onto Murashige and Skoog medium containing 0.8% (w/v) agarose, stratified for 4 d in the dark at 4°C, and then grown at 22°C in continuous white light. Whole plants were harvested after 10 days, and total RNA was extracted with RNeasy Plant Mini Kit (QIAGEN) following the manufacturer's protocols.

To analyze the differential accumulation of transcripts in the nucleus, compared to their abundance in whole cell extracts, a nuclear purification protocol was applied as described by Bologna et al. Mol Cell 2018 [38]. Briefly, Col-0 and *eds4* seeds were sown on Murashige and Skoog medium and then grown at 22°C in continuous white light. Whole plants were harvested after 10 days and fresh tissue was cross-linked and fixed by applying twice vacuum in fixative buffer pH 7.5 (10 mM Tris, 10 mM Na_2EDTA, 100 mM NaCl, 0.1% (w/v) Triton X-100, 1% (w/v) formaldehyde) for 7 min on ice. Glycine was then added to a final concentration of 0.125 M and samples were incubated under vacuum for an additional 7 min on ice. Samples were washed with Tris buffer, dried, and incubated in 1-2 mL of Nuclei Isolation Buffer (15 mM Tris, 2 mM Na_2EDTA, 0.5 mM spermine, 80 mM KCl, 20 mM NaCl, 15 mM β-mercaptoethanol, 0.1% (w/v) Triton X-100) before being chopped finely with a fresh razor blade. The crude homogenate was filtered, and crude nuclear preparations were stained using DAPI and flow-sorted using a BD FACS Aria III cell sorter. After sorting, nuclei were centrifuged for 60 min at 300 g at 4°C, sonicated in a Bioruptor, and reverse cross-linked by 15 min incubation at 50°C and for 30 min at 65°C with NaCl (final concentration 200 mM) and 40 μg of proteinase K. RNA was phenol-extracted, precipitated in sodium acetate, ethanol, and glycogen, washed in 80% (v/v) ethanol and re-suspended in RNase-free water.

To estimate the concentration and quality of samples, NanoDrop 2000c (Thermo Scientific) and gel electrophoresis were used. Libraries were prepared following the TruSeq RNA Sample Preparation Guide (Illumina). Briefly, 3 μg of total RNA was polyA-purified and fragmented; first-strand cDNA was synthesized using reverse transcriptase (SuperScript II; Invitrogen) and random hexamers. This was followed by RNA degradation and second-strand cDNA synthesis. End repair and the addition of a single A nucleotide to the 3′ ends allowed ligation of multiplex indexing adapters. Then, an enrichment step of 12 cycles of PCR was performed. Library validation included size and purity assessment with the Agilent 2100 Bioanalyzer and the Agilent DNA1000 Kit (Agilent Technologies). Samples were pooled to create 12 multiplexed DNA libraries, which were pair-end sequenced with an Illumina HiSeq1500 at INDEAR Argentina, providing 100-bp single end reads. For the differential gene expression analysis, four or three replicates for

each genotype were sequenced and for the analysis of differential retention of transcripts, two replicates for each condition were sequenced. Sequencing data have been uploaded to the Gene Expression Omnibus database and are available under accession number GSE120757.

Processing of RNA sequencing reads

Sequence reads were mapped to *Arabidopsis thaliana* TAIR10 [39] genome using TopHat v2.1.1 [31] with default parameters, except that the maximum intron length was set at 5,000. Count tables for different feature levels were obtained from bam files using custom R scripts (available upon request) and considering the TAIR10 transcriptome.

Differential gene expression analysis

Before differential expression analysis, we decided to discard genes with fewer than 10 reads on average per condition. Differential gene expression was estimated using the edgeR package version 3.4.2 [32] using custom R scripts, and resulting P values were adjusted using a false discovery rate (FDR) criterion [40]. Genes with FDR values lower than 0.10 and an absolute $\log_2$ base two-fold change greater than 0.58 were deemed differentially expressed. Overlapping analysis was performed using BioVenn [33]. Differentially expressed genes (DEGs) in the *eds4* mutant compared to WT Col-0 can be found in Data S1.

In silico validation of nuclei enrichment in nuclear samples

The proportion of unspliced to spliced RNAs of some constitutively spliced genes was evaluated *in silico* to validate nuclear enrichment. The read density of the most distal intron and an adjacent exon was calculated as the number of reads divided by the length of the intron or exon in the transcripts, respectively. This calculation was performed for four different house-keeping genes (ACT2: AT3G18780, ACT7: AT5G09810, ACT8: AT1G49240, GADPH: AT1G13440). The proportion of unspliced to spliced mRNAs, evaluated as intron to exon read density (rd) ratio (expressed as percentage), was then calculated for nuclear only and nuclear plus cytoplasmic (total) samples of the wt genotype. Non-spliced versus spliced actin mRNA levels were enriched, on average, almost 24-fold in nuclei- versus total-cell fractions prepared from wt plants by FACS (Data S2).

Differential nuclear to total transcripts' accumulation

Differential accumulation of transcripts was first determined by performing a differential expression analysis between *eds4* and wt nuclear only samples ($Log_2FC > |0{,}58|$ and FDR $\leq 0{,}15$), resulting in a list of 582 genes. For each of these genes we then estimated an average number of sequencing counts in the nuclear and total samples in wt and *eds4* genotypes. The nuclear to total abundance ratio was calculated for each gene in each genotype (wt and mutant) and then the relation between *eds4* and wt samples was estimated. Transcripts with ratio values > 2 (corresponding to 341 genes) were considered as differentially accumulated in the *eds4* mutant. Differential nuclear/total transcripts' accumulation in the *eds4* mutant compared to wild type Col-0 can be found in Data S2.

Functional category enrichment analysis

Functional categories associated with specific groups of genes were identified using the BioMaps tool from the virtual plant software (http://virtualplant.bio.nyu.edu/cgi-bin/vpweb) and manually cured (Data S1). This tool allowed us to determine which functional categories were statistically over represented in particular lists of genes compared to the entire genome [41]. In each functional category, we determined the genes in common with our datasets, calculating a representation factor and the probability of finding an overlap simply by chance. The representation factor is the number of overlapping genes divided by the expected number of overlapping genes drawn from two independent groups. A representation factor > 1 indicates more overlap than expected by chance for two independent groups of genes, and a representation factor < 1 indicates less overlap than expected. The probability of each overlapping was determined using a hypergeometric probability formula. Gene ontology analysis for differentially expressed genes (DEGs) and differentially accumulated transcripts in the *eds4* mutant compared to wild type Col-0 can be found in Data S1 and S2.

Estimation of nuclear to total ratio

An average number of sequencing counts in each of the sequenced gene transcripts was determined for the nuclear and total samples in both wt and *eds4* genotypes. Then, the nuclear to total abundance ratio was calculated for each gene in each genotype, and averages for the whole genome and different gene ontologies or functional categories were estimated. Nuclear to total ratio of sequencing counts for core clock gene transcripts in wt Col-0 and *eds4* samples can be found in Data S2.

Differentially expressed genes 1 h post infection

Differentially expressed genes (DEG) in wt Col-0 plants treated with virulent *Pseudomonas syringae* pv tomato DC3000 strain in contrast with mock treatment (MgSO4 10mM) at 1 post inoculation were obtained from publicly available RNA-seq data from Howard, Hu et. al. [21]. A list of the DEGs in wt Col-0 plants 1 h post-infection (h.p.i) can be found in Data S3.

Quantitative PCR analysis of circadian clock gene expression at 1 h.p.i

Plants were grown in SD conditions for 5-6 weeks and then an infection protocol similar to the one performed in the bacterial growth assays was implemented for inoculation with *Pseudomona syringae* pv. *tomato* DC3000 (OD_{600} = 0.002) or mock solution (10 mM $MgCl_2$) at ZT = 2. Tissue was harvested 1 h.p.i. Leaves from two different plants were pooled in each sample to reduce

biological variation and three samples per genotype and treatment were obtained. Total RNA was extracted using TRIzol reagent (Invitrogen) according to the manufacturer's protocol. One microgram of RNA was treated with RQ1 RNase-Free DNase (Promega) and subjected to retro transcription with Super Script II Reverse Transcriptase (Thermo Fisher Scientific) and oligo-dT, according to manufacturer's instructions. cDNAs were then amplified with FastStart Universal SYBR Green Master (Roche) using the Mx3000P Real Time PCR System (Agilent Technologies) cycler. The IPP2 (AT3G02780) transcript was used as a housekeeping gene. Quantitative RT-PCR (qRT-PCR) analysis was conducted using the standard curve method as described in the Methods and Applications Guide from Agilent Technologies. Results were calculated relative to IPP2 transcript levels and indicate mean values relative to mock-treated WT plants in 2 independent experiments. Primers sequences used are summarized in Table S1.

Quantitative PCR analysis of circadian clock gene expression in SD

Plants were grown in SD conditions for 2 weeks and then whole young plants were harvested every 4 h during 24 h. The 100mg of green tissue from each time point was pooled in each sample and three samples per genotype were obtained. Total RNA was extracted using TRIzol reagent (Invitrogen) according to the manufacturer's protocol. One microgram of RNA was treated with RQ1 RNase-Free DNase (Promega) and subjected to retro transcription with Super Script II Reverse Transcriptase (Thermo Fisher Scientific) and oligo-dT, according to manufacturer's instructions. cDNAs were then amplified with FastStart Universal SYBR Green Master (Roche) using the Mx3000P Real Time PCR System (Agilent Technologies) cycler. The IPP2 (AT3G02780) transcript was used as a housekeeping gene. Quantitative RT-PCR (qRT-PCR) analysis was conducted using the $2^{-\Delta\Delta CT}$ method [42]. Primers sequences used are summarized in Table S1.

QUANTIFICATION AND STATISTICAL ANALYSIS

Statistical analysis was performed using GraphPad Prism 6 (GraphPad Software). The values shown in the figures are either means of biological replicates or means of independent experiments, as specified in each figure caption. Details of statistical tests applied are indicated in figure legends including statistical methods, number of biological replicates, number of individuals, mean and error bar details, and statistical significances.

DATA AND CODE AVAILABILITY

The whole genome sequencing datasets supporting the results of this article are available in the Sequence Read Archive (SRA). The accession number for the data reported in this paper is SRA: PRJNA493644. https://www.ncbi.nlm.nih.gov/sra/PRJNA493644

The RNA-seq datasets supporting the results of this article are available in the Gene Expression Omnibus (GEO) repository. The accession number for the data reported in this paper is GEO: GSE120757. https://www.ncbi.nlm.nih.gov/geo/query/acc.cgi?acc=GSE120757.